

## APPLICATION OF NON-THERMAL PLASMAS TO GAS CLEANING AND ENHANCING COMBUSTION FOR POLLUTION REDUCTION

**L.A. ROSOCHA & Y. KIM**

Los Alamos National Laboratory

[rosocha@lanl.gov](mailto:rosocha@lanl.gov)

### ABSTRACT

For more than two decades, interest in gas-phase pollution control has greatly increased, arising from more attention to the health and economic effects of pollution, a greater respect for the environment, and a larger body of laws and regulations. Non-thermal plasma (NTP) technology shows promise for removing pollutants from gas streams and cleaning contaminated surfaces, using plasma-generated reactive species (e.g., free radicals). Such plasmas, where electrons are energetic (~ few eV) and the gas temperature is near ambient (~ 300 K), can generate both oxidative and reductive radicals - showing promise for treating a variety of pollutants, sometimes simultaneously decomposing multiple species. NTPs can also be used to 'activate' or 'crack' hydrocarbon fuels, which promotes the combustion of the fuels (reducing unburned hydrocarbons and allowing fuel burning in regimes where the emissions of CO and NO<sub>x</sub> are expected to be reduced; e.g., ultra-lean-burn conditions). In this paper, we will review selected experiments and field tests related to the cleaning of VOCs (volatile organic compounds) and NO<sub>x</sub> from gas streams, using NTPs and discuss a particular NTP source for surface decontamination (radionuclides and chemical/biological warfare agents). The remainder of the paper will focus on experiments devoted to non-thermal plasma-assisted combustion, using model gaseous fuels (like methane, propane, and butane) and alluding to the possibility of applying the process to liquid fuels (like iso-octane, a gasoline surrogate). We will present experimental results demonstrating that NTPs can affect flame stability and, in this way potentially reduce the emission of pollutants.

## **INTRODUCTION**

### **Motivation for Research**

Over the past two decades, there has been considerable interest in applying NTPs to hazardous chemical destruction, pollution control, and surface decontamination, as described in Penetrante & Schultheis (1993), van Veldhuizen (2000), and Rosocha (2005). Such applications include the treatment of hydrocarbons and halocarbons (many solvents) entrained in soil and water or emitted as stack gases, and oxides of nitrogen (nitric oxide NO, in particular) in flue and engine-exhaust gases. Surface decontamination applications have also included actinides, as discussed by Rosocha (2005) and chemical and biological warfare (CBW) agents, as described by Herrmann et al (1999). NTPs have also been applied to combustion, mainly for two reasons: attempts to increase combustion efficiency and improving combustion stability for the reduction of pollutant emissions; see Rosocha et al (2004, 2005) and Cha et al (2005).

### **Definition and Advantages of Non-Thermal Plasmas**

Non-thermal plasmas (NTPs) - sometimes called non-equilibrium or 'cold' plasmas - have different electron, ion, and neutral species temperatures; the electrons have the highest temperature (e.g., 1-10 eV). Such plasmas are good sources of highly reactive oxidative and reductive species, e.g.,  $O(^3P)$ , OH, N, H, NH, CH,  $O_3$ ,  $O_2(^1\Delta)$ , and plasma electrons. Via these species, one can direct electrical energy into favorable gas chemistry (like decomposing pollutants or fragmenting larger hydrocarbons into smaller, more-easily combustible ones). Operating an NTP reactor at atmospheric pressure provides much greater processing rates and throughput than low-pressure reactors. Atmospheric-pressure NTPs can be easily created by electrical discharges in a variety of gases (including air), as described in Penetrante & Schultheis (1993), Rosocha (1997), van Veldhuizen (2000), and Barker et al (2005).

Direct-current (DC) and pulsed coronas, dielectric barrier discharges (DBDs), and RF-driven discharges are convenient plasma sources for these applications. The book of Veldhuizen (2000) is a good source for current research using electrical discharges, as applied to gas-phase pollution control. Electron-beam-generated NTPs are also useful for pollutant destruction, as shown by Slater & Douglas-Hamilton (1981) and described in the workshop proceedings of Penetrante & Schultheis (1992), but are out of the scope of this paper.

## **REPRESENTATIVE NTP REACTORS**

### **Background**

In this section, we will discuss four representative atmospheric-pressure NTP reactors for pollutant destruction: DC corona, pulsed corona, dielectric-barrier (also called silent discharge), and RF plasma jet. The first three reactors all share a common trait, namely operating in the streamer-discharge mode described by Raether (1964), while the RF plasma jet operates in a quasi-glow-discharge regime (normally because it incorporates rare-gas additives), as described by Herrmann et al (1999) and Barker et al (2005).

The main reason that streamer-based reactors, discussed in Veldhuizen (2000), Penetrante & Schultheis (1992), Rosocha (1997), and Barker et al (2005), are so useful is that the streamer is prevented from becoming an arc (thermal plasma) by the spatio-temporal distribution of the electric field. For DC corona, electrode geometry and space charge buildup around a point or wire governs fall-off of the electric field. For pulsed corona, both electrode geometry and the use of short pulses combine to restrict reactor operation to non-thermal plasma conditions.

For dielectric-barrier devices, physical charge buildup on a dielectric surface provides an arc-counteracting electric field that ensures non-thermal discharge behavior. These three related cases are all self-terminating electric discharges. In general, electric-discharge streamers at atmospheric pressure can be thought of as cylindrical current filaments with typical radius  $\sim 100 \mu\text{m}$ . They are transient discharges (e.g., lasting only a few nanoseconds for oxygen or air), fed by ionization and detachment and then arrested when the electric field is reduced to the point where electron attachment becomes dominant. For streamers in pure oxygen and air, the average electron energy and electron density are  $T_e \sim 3\text{-}5 \text{ eV}$ ,  $[e] \sim 10^{14}/\text{cm}^3$ , while a typical breakdown reduced electric field strength (electric field magnitude divided by total process gas pressure) in the gas is  $E/N \sim 100\text{-}200 \text{ Td}$ .

An RF-driven plasma jet maintains non-thermal properties by preventing glow-to-arc transitions via an oscillating electric field and the inclusion of rare gases in the reactor process stream (which also act to prevent discharge instabilities).

### **DC Corona Reactor**

In this section, we describe an advanced form of DC corona reactor for  $\text{NO}_x$  destruction, described by Chang et al (1999). In this configuration (see Figure 1), needle-plane corona discharges are employed to create  $\text{NO}$  and  $\text{NO}_2$ -decomposing species in a flowing exhaust gas, but with ammonia ( $\text{NH}_3$ ) being injected through hollow corona needles to generate additional radicals (e.g.,  $\text{N}$ ,  $\text{NH}$ ) that are effective in decomposing oxides of nitrogen. A trailer-portable test rig based on this so-called “Corona Radical Shower (CRS)” technique was fielded at the US Tinker Air Force Base to examine the feasibility of treating  $\text{NO}_x$  effluents from jet engine test cells (JETCs).

The field-test CRS NTP reactor treated a small portion of the engine exhaust. It consisted of six parallel-flow, aluminum-plate, channels, each measuring 10 cm wide x 60 cm high x 125 cm long. Each flow channel contains two  $\text{NH}_3/\text{N}_2$  injection-gas manifolds (to feed gas from both top and bottom) and an injection-nozzle array. Each array consists of six 0.375 in (9.5 mm) OD nozzle pipes that hold 56 stainless steel injection nozzles (short lengths of hypodermic needle material) of 0.998 mm ID that protrude approximately 4 mm transverse to the nozzle pipes and perpendicular to the gas flow direction. The nozzle pipes are electrically insulated from ground and connected to a 50 kV/85 mA, positive-polarity high voltage power supply that drives the electrical corona discharge. The project results, described by Urashima et al (1999) and Rosocha et al (2000), which included economic comparisons of various de- $\text{NO}_x$  technologies, demonstrated that the CRS technique was superior to conventional and other plasma de- $\text{NO}_x$  technologies. Figure 2 shows a plot of the field-test de- $\text{NO}_x$  characteristics.

### **Pulsed Corona and Dielectric-Barrier Discharge Reactors**

Here, we will review some representative laboratory-scale pulsed corona reactor (PCR) and DBD reactor experiments carried out on the decomposition of the example hydrocarbon methyl ethyl-ketone (MEK) and the halocarbon trichloroethylene (TCE). Nitric oxide ( $\text{NO}$ ) experiments were similar and are described elsewhere by Rosocha & Korzekwa (1999, 2000). A VOC-removal field test will also be briefly described. Figure 3 shows simple schematic diagrams of DBD and pulsed corona reactors for gas-phase pollutant removal. A high voltage is applied across the electrodes in the gas to create energetic plasma electrons in the electrical discharges. Detailed descriptions of the experimental apparatus have been previously described, in the above citations.

The PCR tests used a wire-tube reactor geometry (stainless steel corona wire with a diameter of 500  $\mu\text{m}$  and a stainless steel tube with an inner diameter of 2.5 cm as the outer conductor and active length of 90 cm). High-voltage pulses (duration < 50 ns; peak voltage 30 kV, repetition rate 1 kHz) were delivered to the wire to create an NTP in the process gas, at a plasma energy of  $\sim 60$  mJ/pulse.

The DBD reactor was of flat-plate geometry using two Pyrex plates with a gap spacing of 3.5 mm. Aluminum plates on either side of the dielectric provide a discharge area of 1800  $\text{cm}^2$ . The power source is a variable-frequency voltage source and a high voltage step-up transformer. The typical operating frequency was 1.2 kHz, but could be changed to produce variable discharge powers up to 350 W. Circuit schematics for the PCR and DBD reactors are shown in Figure 4.

Deposited power in the PCR is measured using a capacitive voltage probe and a current-viewing resistor. Deposited power for the DBD reactor is measured with a voltage probe and charge-measuring capacitor, following the method of Manley (1943), which is more-recently described by Rosenthal & Davis (1975). The plasma specific energy (energy/unit volume) is given by dividing the deposited energy in one residence time by the reactor volume, or the plasma power  $P$  by the process gas flow  $Q$ , for the PCR and DBD reactors, respectively. The proposed chemical-kinetic decomposition pathways and chemical diagnostics, which measured VOC decomposition by gas-chromatograph mass-spectrometer (GC/MS) techniques, are described elsewhere by Rosocha & Korzekwa (1999, 2000).

The removal of two VOCs, trichloro-ethylene (TCE) and methyl-ethyl ketone (MEK), in room-temperature dry air, using the above reactors, was measured. The degree of removal  $[X]/[X]_0$  is plotted as a function of plasma specific energy  $E$  (or, equivalently  $P/Q$ ). As shown in Figure 5 (left), for 200 ppm of TCE, there is no noticeable difference in the removal fraction, using either PCR or DBD, for energy densities up to 400 J/std lit ( $[X]/[X]_0 \approx 0.015$ ). Figure 5 (right) is a removal plot for 1000 ppm of MEK. For energy densities up to 1500 J/std lit, there is no distinguishable difference in the degree of removal, comparing the two reactors. However, for higher energy densities there is a slight difference attributed to a difference in gas temperature in the PCR. This affects both the rate of decomposition reactions and the gas density (which increases the breakdown  $E/N$  at higher temperature). The fact that pollutant destruction in both types of reactors is similar is explained in light of the dependence of the radical-production yields on the breakdown  $E/N$  of the reactors (higher  $E/N$  for PCR, but radical yield falling at higher  $E/N$ ); see Rosocha (1997), Rosocha & Korzekwa (1999, 2000), Kim et al (2004), and citations therein.

### **VOC-Removal Field demonstration at McClellan AFB**

In 1995, a DBD-reactor, VOC-removal technology-demonstration was carried out at McClellan Air Force Base in Sacramento, California. The test site was a former ground-disposal facility for a variety of solvents, volatile, and semi-volatile chemicals (> 50 compounds), including TCE, 1,1,1-TCA, PCE, 1,1,1-dichloroethylene (1,1,1-DCE), benzene, toluene, ethyl-benzene, xylenes, Freon 113 (a chloro-fluorocarbon), methylene chloride, vinyl chloride, and acetone. At the site, the compounds were vacuum extracted from the ground and a portion of the vapor-laden air stream (with VOC concentrations  $\sim 300 - 1000$  ppmv) was sent to the unit illustrated in Figure 6. The demonstration achieved the overall goal of destroying the total VOC concentration by > 95%, at gas flows as high as 10.4 SCFM (295 std lit/min) and achieved a total DRE as high as 99.4% in some cases. See Rosocha et al (1996) for more information on this demonstration.

### **RF-Driven Atmospheric-Pressure Plasma Jet for Decontamination**

The atmospheric-pressure plasma jet (APPJ), shown in Figure 7 is a non-thermal, glow-discharge plasma operating at atmospheric pressure and 13.56 MHz radio frequency, as described by Herrmann et al (1999), Rosocha (2005) and Kim et al (2005a). The discharge uses a feedgas consisting primarily of an inert carrier gas, such as He, and a small amount of an additive to be activated, such as O<sub>2</sub>, CF<sub>4</sub>, or H<sub>2</sub> (that yield active species to destroy organic compounds, CBW agents, or volatilize actinides). Reactive species can be directed onto a contaminated surface at high flow, where they can selectively neutralize organic materials without damaging the underlying surface. The exit gas temperature typically ranges from 50 to 300 C, allowing for plasma processing of sensitive materials and equipment at low temperature, as well as accelerated processing of more robust surfaces that can withstand higher temperatures.

Near-atmospheric pressure NTPs can provide a convenient, waste-free and fast-processing method for the decontamination of numerous substrates and the recovery of residual quantities of plutonium and other actinides that form volatile fluorides. Plasmas have been demonstrated to effectively decontaminate actinide-contaminated surfaces through production of atomic fluorine, which etches metal and metal oxide surfaces. In the case of Pu, volatile PuF<sub>6</sub> is produced which can then be pumped away and captured in a variety of filtering techniques.

In APPJ-etching studies, further described in Rosocha (2005) and contained citations, 1/8-in.-thick, 1-in.-diameter stainless steel coupons (disks) were impregnated with small amounts of plutonium and uranium and then exposed to an APPJ effluent. The 13.56-MHz APPJ was operated at 700 W. About 90% of the uranium was removed in 10 minutes, whereas about 50% of the plutonium was removed in the same amount of time. The plutonium-doped coupons were further exposed at 10-minute intervals. This Pu-removal data is shown in Figure 8.

The APPJ was also tested to destroy biological warfare agent surrogates, chemical warfare agent surrogates, as well as actual chemical warfare agents, as shown by Herrmann et al (1999). Active species produced inside the APPJ plasma (typically using He/O<sub>2</sub> feedgas) are rapidly blown out of the source to the target surface, 2-10 mm downstream. Typically, decontamination of *Bacillus globigii* (BG), a simulant for Anthrax spores, with APPJ effluent was ~ 10 times faster than dry heat. The APPJ was also demonstrated to effectively decontaminate surrogates for sulfur mustard and VX nerve agent (e.g., pesticide Malathion), as well as actual VX.

### **PLASMA-ASSISTED COMBUSTION WITH DBDs**

In this section, we will discuss some of our experiments, as further discussed by Kim et al (2005b), on the influence of plasma excitation on the blowout limit of an activated-propane/air flame (i.e., ultra-lean-burn conditions). A schematic of the experimental setup is shown in Figure 9. Air flows through a grounded tubular inner electrode (diameter 0.96 cm). Propane (C<sub>3</sub>H<sub>8</sub>) flows through the annular gap between the inner electrode and an alumina ceramic tube (inner diameter 1.9 cm). This configuration, with the air surrounded by fuel, is called an inverse flame. The ceramic tube is surrounded by a cylindrical metal outer electrode, which is powered by a HV AC transformer. The applied AC frequency was tuned to about 450 Hz, which matched the impedance of our propane DBD. Thus, power was applied to the propane but not the air, activating the fuel. The inner electrode is shorter than the ceramic tube, so there is a region (of variable length, but generally < 14 mm) where the

fuel and air partially mix before being ignited. The power deposited into the plasma was measured using Lissajous diagram techniques (charge-voltage plot), as presented in Manley (1943) and Rosenthal & Davis (1975).

We conducted blowout tests by holding the propane flow constant and increasing the air flow rate until the flame blew out. The blowout air flow rate is an indicator of flame stability, and a high blowout air flow rate shows that combustion continues to occur under lean-burn conditions. Most notably, the strongest plasma effect is increased stability at large air flows. Figure 10 shows the minimum blowout air flow rates of an inverse, partially premixed flame for propane flow rates between 0.2 and 0.8 lpm. The results (air flow vs propane flow) are parameterized according to the equivalence ratio  $\phi$  for propane-air combustion, given in Nylund & Lawson (2000)

$$f = \frac{15.6 \times (\text{propane flow rate}) \times (\text{propane density})}{(\text{air flow rate}) \times (\text{air density})},$$

which is a standard combustion metric. In the absence of a plasma, the blowout limit of a propane flame increases with the propane flow rate and begins to saturate at 0.6 lpm propane. When 10 W discharge power is applied to the fuel, the blowout limit shows a large increase for low propane flow (and low equivalence ratio). However, the plasma benefit decreases as the propane flow increases, and for propane flow  $> 0.6$  lpm the blowout rate actually decreases in the presence of a plasma. This is not necessarily detrimental, because low-equivalence-ratio systems show large decreases in pollutant production, especially NO<sub>x</sub>, and are of great interest. In this experiment, the discharge power was held constant (10 W) while the propane flow rate was increased. Thus, the discharge energy density  $\epsilon$ ,

$$e = \frac{\text{discharge power}}{\text{gas flow rate}},$$

deposited into the propane decreased as the propane flow rate increased. For example, at a propane flow rate of 0.3 lpm,  $e = 2$  kJ/std lit, while at a propane flow rate of 0.8 lpm, the  $e$ -value fell to 0.75 kJ/std lit. Thus, the magnitude of the discharge energy density seems to affect the blowout limit of a propane flame. In the future, more experiments will be performed to correlate the combustion enhancement with the discharge energy density.

## ACKNOWLEDGMENTS

The authors appreciate background work and technical assistance from J. Coogan, R. Korzekwa, G. Anderson, H. Herrmann, J. Park, G. Selwyn, S. Stange, V. Ferreri, and S. Abbate.

## REFERENCES

- Barker, R., Becker, K., U Kogelschatz, and K. Schoenbach, editors (2005). *Non-Equilibrium Air Plasmas at Atmospheric Pressure*, Institute of Physics Publishing, London, Bristol, Philadelphia, Tokyo, Beijing.
- Cha, M.S., Lee, S.M., Kim, K.T., and Chung, S.H. (2005). *Soot suppression by nonthermal plasma in coflow jet diffusion flames using a dielectric barrier discharge*, Combustion and Flame, **141**, pp.438-447.

- Chang, J-S, Tan, M-T, Cheng, Z. and Tong, Y-C (1999). *Simultaneous removal of NO<sub>x</sub> and SO<sub>2</sub> from NO-SO<sub>2</sub>-CO<sub>2</sub>-N<sub>2</sub>-O<sub>2</sub> gas mixtures by corona radical shower systems*, J. Phys. D: Appl. Phys., **32**, pp. 1006-1011.
- Herrmann, H.W., Henins, I., Park, J., Selwyn, G.S. (1999). *Decontamination of chemical and biological warfare (CBW) agents using an atmospheric pressure plasma jet (APPJ)*, Phys. Plasmas, **6**, pp. 2284-2289.
- Kim, Y., Kang, W.S., Park, J.M., Hong, H.S. Song, Y.H. and Kim, S.J. (2004). *Experimental and Numerical Analysis of Streamers in Pulsed Corona and Dielectric Barrier Discharges*, IEEE Trans. Plasma Sci. **32**, pp. 18-24.
- Kim, Y., Park, J., Rosocha, L.A., Teslow, H.L., Herrmann, H.W (2005a). *Measurements of dioxygen fluoride (O<sub>2</sub> F) in an atmospheric pressure plasma jet*, Appl. Phys. Lett.; **87**, pp.1-3.
- Kim, Y; Stange, S.M.; Rosocha, L.A.; Ferreri, V.W. (2005b). *Enhancement of propane flame stability by dielectric barrier discharges*, J. Adv. Oxid. Technol., **8**, pp.188-192.
- Manley, T.C. (1943). *The Electrical Characteristics of the Ozonator Discharge*, Trans. Electrochem. Soc. **84**, pp. 83-95.
- Nylund, N.O. and Lawson, A. (2000). *Exhaust Emissions from Natural Gas Vehicles*, International Assoc. for Natural Gas Vehicles, Sigma Group, Takapuna, New Zealand.
- Penetrante, B.M. and Schultheis, S.E. (1993). *Proceedings of NATO Advanced Research Workshop on Non-Thermal Plasma Techniques for Pollution Control, Series G: Ecological Sciences, Vol. 34, Parts A&B*, Springer-Verlag, Berlin, Heidelberg, New York.
- Raether, H. (1964). *Electron Avalanches and Breakdown in Gases*, Butterworths, London.
- Rosenthal, L.A. and Davis, D.A. (1975). *Electrical characterization of a corona discharge for surface treatment*, IEEE Trans. Industry Appl. **IA-11**, pp. 328-334.
- Rosocha, L.A. (1997). *Processing of Hazardous Chemicals Using Silent Electrical Discharge Plasmas*, in Environmental Aspects in Plasma Science, edited by Manheimer, W., Sugiyama, L.E., and Stix, T.H., American Institute of Physics Press, Woodbury, New York.
- Rosocha, L.A., Coogan, J.J., Korzekwa, R.A., Secker, D.A., Reimers, R.F., Herrmann, P.G., Chase, P.J., Gross, M.P. and Jones, M.R. (1996). *Field Demonstration and Commercialization of Silent Discharge Plasma Hazardous Air Pollutant Control Technology*, Proc. 2<sup>nd</sup> Int. EPRI/NSF Symp. on Environmental Applications of Advanced Oxidation Technologies, Electric Power Research Institute, Palo Alto, CA, pp. 5-17.
- Rosocha, L.A. and Korzekwa, R.A. (1999). *Advanced Oxidation and Reduction Processes in the Gas Phase Using Non-Thermal Plasmas*, J. Adv. Oxid. Technol., **4**, pp. 247-264.
- Rosocha, L.A., Miziolek, A.W., Nusca, M.J., Daniel, R.G., Chang, J-S, Urashima, K, Looy, P.C., Herron, J.T. and Huie, R.E. (2000). *Development of Non-Thermal Plasma Reactor Technology for Control of Atmospheric Emissions: Final Report for SERDP Project CP-1038*, Los Alamos National Laboratory Report, LA-UR-00-4479.

Rosocha, L.A., Platts, D., Coates, D.M. and Stange, S. (2004). *Plasma-Enhanced Combustion of Propane Using a Silent Discharge*, *Physics of Plasmas*, **11**, pp. 2950-2956.

Rosocha, L.A. (2005). *Non-Thermal Plasma Applications to the Environment: Gaseous Electronics and Power Conditioning*, *IEEE Trans. Plasma Sci.* **33**, pp. 129-137.

Rosocha, L.A., Kim, Y. and Stange, S. (2005). *Application of a Non-Thermal Plasma to Combustion Enhancement*, *Proc. 6<sup>th</sup> Institute Electrostatics of Japan – Electrostatics Society of America Joint Symposium*, pp. 367-374.

Slater, R.C. and Douglas-Hamilton, D.H. (1981). *Electron-beam-initiated destruction of low concentrations of vinyl chloride in carrier gases*, *J. Appl. Phys.*, **52**, pp. 5820-5828.

Urashima, K., Tong, X., Chang, J-S, Miziolek, A. and Rosocha, L.A. (1999). *Acid Gas Removal Characteristics of Corona Discharge Methane Radical Shower-Catalyst Hybrid System for Treatment of Jet Engine Test Cell Flue Gas*, *Proceedings of 1999 SAE International Fuels & Lubricants Meeting*, paper 99FL-258.

Van Veldhuizen, E.M., editor (2000) *Electrical Discharges for Environmental Purposes - Fundamentals and Applications*, Nova Science Publishers, Inc., Huntington, New York.

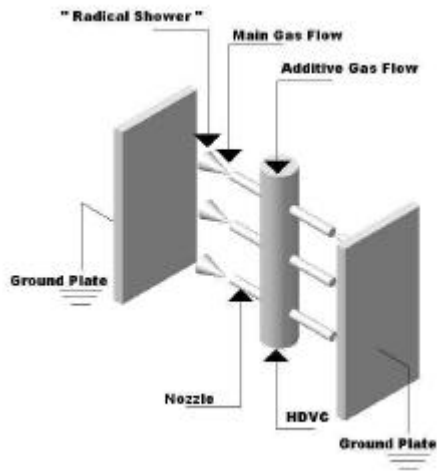


Fig. 1: Schematic diagram of the CRS reactor concept for  $\text{NO}_x$  removal in exhaust gas.

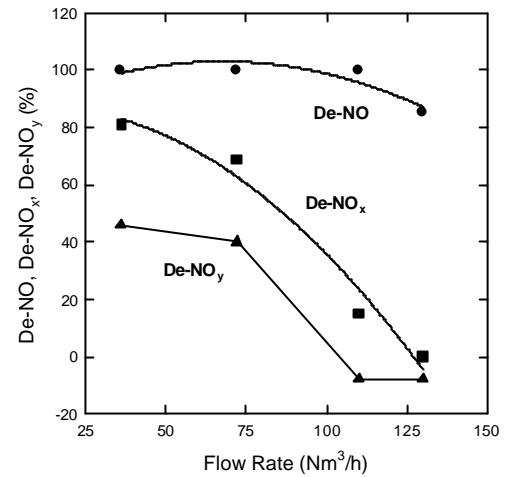


Fig. 2: Removal plot for oxides of nitrogen, as obtained from a field demonstration on jet engine test cell exhaust (carried out at Tinker Air Force Base, USA).

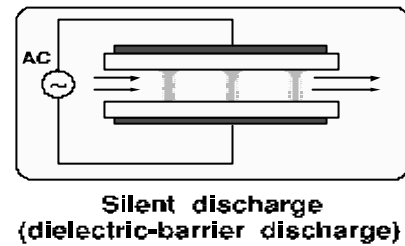
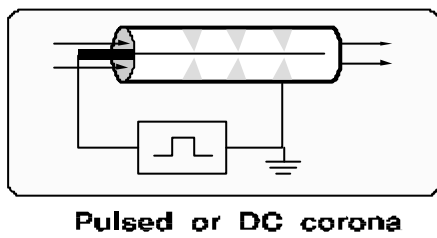


Fig. 3: Schematic diagrams of example pulsed corona (left) and dielectric-barrier discharge (right) reactors.

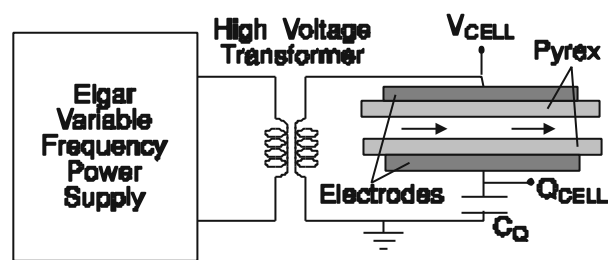
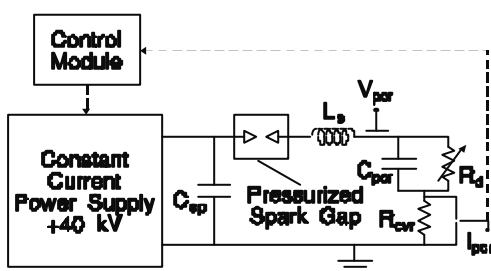


Fig. 4: Circuit schematic diagrams of typical pulsed corona (left) and flat-plate, dielectric-barrier discharge (right) reactors employed in our experiments.

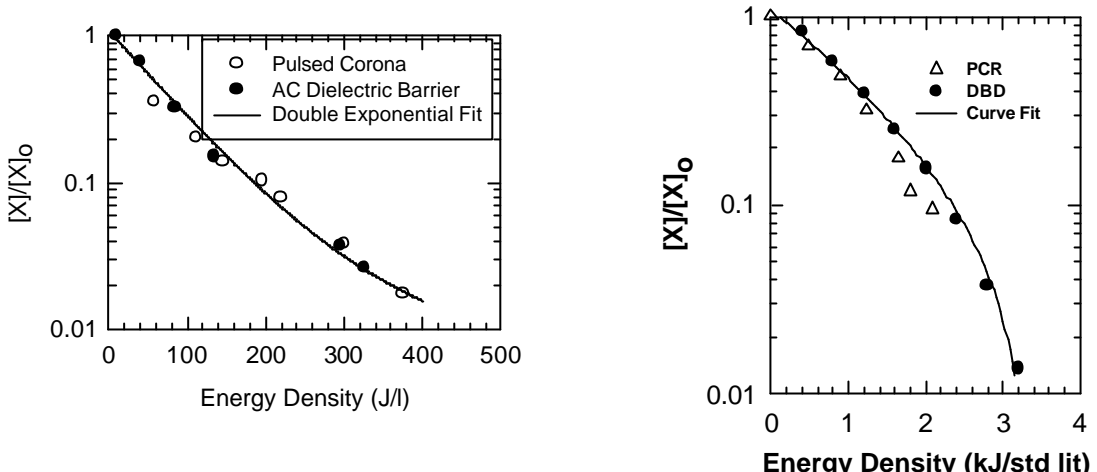


Fig. 5. Removal plots for TCE (left) and MEK (right), for both PCR and DBD plasma reactors.

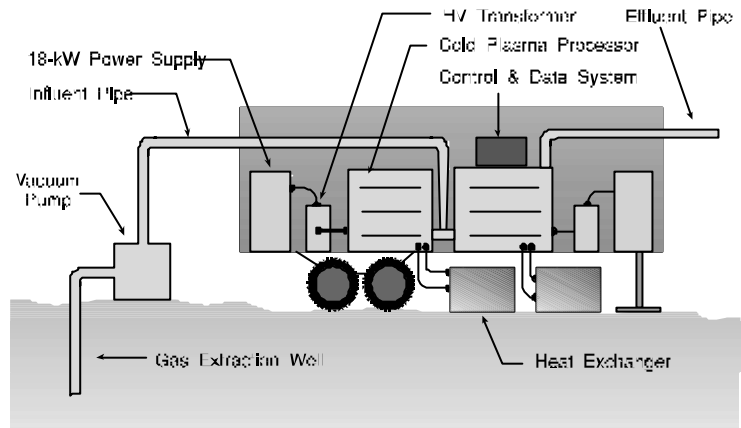


Fig. 6: Artist's conception of the mobile, DBD-based system for the destruction of vapor-extracted VOCs from soil at the US McClellan Air Force Base.

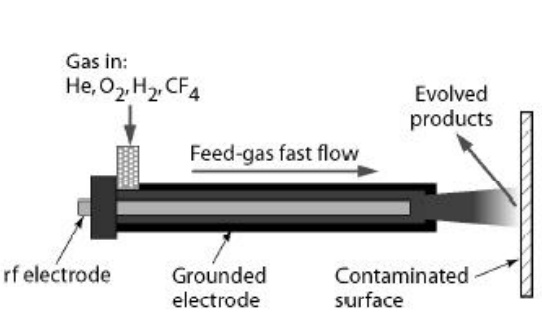


Fig.7: Schematic diagram of a cylindrical RF-powered atmospheric-pressure plasma jet.

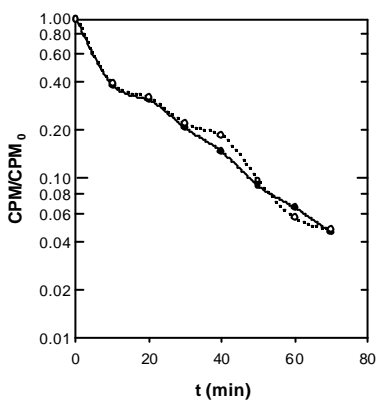


Fig.8: Plot of APPJ decontamination of Pu-doped coupons (counts/min relative to original activity versus time), using two different detectors.

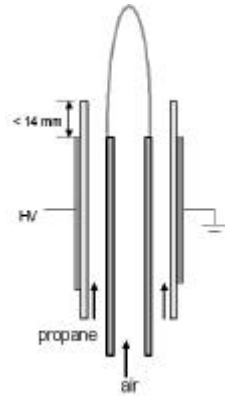


Figure 9: Schematic diagram of burner incorporating DBD plasma excitation of propane for enhanced combustion.

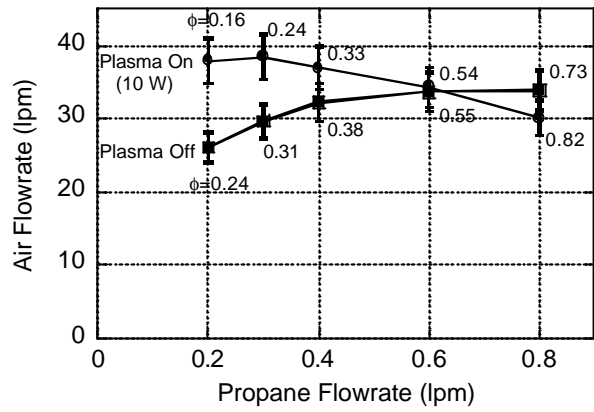


Figure 10: Blowout plot of lean-burn combustion of propane, enhanced by plasma activation.